Research on the Surface Deformation Law with the Mining Process of Tangjiazhuang Iron Mine Based on FLAC^{3D}

Chi Zhang[1, 2, a, *], Yin Chen[3, b], Ping Liu[4, c], Hu Ji[1, 2, d], Jinyang Li[1, 2, e]

[1]BGRIMM Technology Group, Beijing, China

[2]National Centre for International Research on Green Metal Mining, Beijing, China

[3]Xinjiang Xinxin Mining Co., Ltd., Urumqi, China

[4]Jinning Ore Dressing Subsidiary of Yunnan Phosphate Group Co., Ltd., Kunming, China

[a]zhangchi@bgrimm.com, [b]xjyscy@163.com, [c]742109475@qq.com, [d]jihu@bgrimm.com, [e]lijinyang@bgrimm.com

* Corresponding Author Email

Abstract. In view of the current situation that the mining process of underground mines is easy to induce surface deformation, which leads to cracking and deformation of surface structures, this paper uses finite difference numerical analysis software FLAC3D to establish a fine engineering geomechanical model of Tangjiazhuang Iron Mine. Combined with the overall plan of ore recovery in each middle section of the mine, the production status of the current stage of the mine is simulated and the rationality of the three-dimensional numerical calculation model is verified by the deformation characteristics of typical surface structures in the mining area. on this basis, the paper simulates the general law of surface deformation under waste rock filling mining for the next mining planning scheme of +113m and +69m in the middle section of the mine. on the one hand, it explains the surface deformation characteristics induced by the mining process as a whole. on the other hand, it also further explains the actual situation that the surface deformation induced by sublevel stoping with subsequent waste rock filling will not have a great impact on the surface structures, which lays a foundation for orderly organizing production, reasonable arrangement of mining sequence and prevention of surface deformation in the later stage of the mine.

Keywords: Underground mine, Stoping process, Surface deformation, The numerical simulation.

1. Introduction

Underground mining of metal mines is a typical mining type that realizes the recovery of ore with a certain buried depth through drilling and lifting transportation engineering to reach the ore body[1]. With the shrinking of shallow metal mine resources in China, underground mining has become the main way of ore recovery for a long time. As underground mining is a process in which stress is released by excavation and then the regional geostress field is redistributed[2-3], the formation of goaf is bound to show typical geopressure problems such as roof subsidence, floor heave and side slope under the complex action of overlying rock self-weight stress and regional horizontal tectonic stress. With the gradual increase of the mining area, the performance characteristics of the above problems are further intensified and extended to the surrounding areas, and are shown as settlement and inclined deformation[4]in the surface area. Slight deformation is difficult to be identified by the naked eye, but when the local deformation exceeds a certain limit, it is difficult to detect the surface deformation. The surface and even structures will show relatively obvious cracking[5-6], which will affect the life and property safety of the surface industrial site and even the surrounding people. Therefore, it is of great significance to carry out surface deformation analysis in the mining process of metal mines to ensure the steady implementation of mining work and ensure the safety and stability of the surrounding people.

Many scholars at home and abroad have carried out a lot of effective research work on the surface deformation in the process of underground mining. Among them, Wang Wei et al.[7]analyzed the key role of determining dimension safety pillar for the safety and stability of surface filling station by using three-dimensional modeling and finite difference software combined simulation calculation for the surface settlement problem in the mining process of a large underground iron mine, and further determined the optimal pillar size through comparative analysis. Cao Wenlong et al.[8]used ANSYS and FLAC^{3D}software to simulate and analyze the surface rock movement and influence range caused by underground mining in view of the impact degree and scope of subsequent mining in an underground mine on surface buildings and main shafts. It is concluded that the underground mining mainly affects the vertical rock mass of the roof of the orebody when the safety pillar of a certain size is left. Liu Huanchun et al.[9]used ABAQUS finite element software to study rock mass deformation and surface movement caused by filling mining in metal mines, aiming at the problem that surface deformation caused by underground mining affects the safety of surface buildings. They found that the mechanical strength of surrounding rock is higher, the roof subsidence caused by mining is less, and the filling action can restrain floor heave. The conclusion that the surface deformation is mainly concentrated in the middle of the goaf; Guo Yanhui et al.[10]used discrete element 3DEC software to analyze the movement and deformation laws of the surface and surrounding rock caused by mining of the ore body under the same tectonic stress environment when the ore body inclination is 50°, 60°, 70°, 80° and 90° respectively. It is concluded that the maximum subsidence deformation decreases with the increase of the dip Angle. Wang Rui et al.[11]used differential synthetic aperture radar technology to conduct cumulative temporal deformation monitoring of the mining area, which better identified the small-scale deformation area within the mining area and extracted the subsidence basin boundary, in view of the low deformation resolution predicted by the traditional surface deformation monitoring with limited points. Peng Dingxiao et al.[12], aiming at the delineation of surface movement zone in Hongling lead-zinc mine, established a prediction model of mine movement Angle with caving method by combining PSO-SVM algorithm with numerical simulation, and obtained a reasonable range of surface movement zone through mutual verification. It provides a new method for delineating the surface moving zone of metal mines. Wu Yabin et al.[13]took a large copper-nickel mine as the research object and compared the influence of overburden movement and surface deformation under three different mining sequences through simulation, aiming at the surface deformation that may be induced by open-stope subsequent filling mining process. It is found that the difference of surface deformation gradually decreases with the increase of mining depth, and the most prominent mining depth under corresponding mining conditions is determined. Ye Wei et al.[14]established an observation station for surface movement and deformation of the working face under the condition of repeated mining, aiming at the problem that a large area of surface subsidence water is formed on the surface due to repeated mining, and obtained that the fractures located in the first stretching and then compression deformation zone during the mining process show a dynamic evolution process from generation to development and then to closure. In summary, various scholars have carried out rich and detailed research on the research objects under different working conditions, which provides a basis for more comprehensive and accurate research on the surface deformation law in the mining process.

Taking Guangfeng Tangjiazhuang Iron Mine in Chengde as the research object, this paper adopts FLAC^{3D}numerical simulation software to first simulate and analyze the surface deformation characteristics at the current stage of the mine, and then makes a comparison and verification with the mine status. On the basis of ensuring the initial conditions, the mining process of the deep ore body is simulated according to the established mining mode and sequence. The analysis of surface deformation characteristics provides a reliable basis for the mine to rationally arrange the mining mode and sequence and ensure the normal production of the mine.

2. Mine Engineering Overview

The main mining orebodies of Tangjiazhuang Iron Mine include Fe4 and Fe22 orebodies. The Fe4 orebody is located in the west of the mining area with a length of 1100m, an average thickness of 9.36m and a maximum extension of 453m. The orebody strikes 70°, has a dip of 340° and an inclination of 67°, and the occurrence elevation of the orebody ranges from 532 to 72m. The orebody No. Fe22 is located in the middle of the mining area. The orebody length is 434m, the average thickness is 4.23m, the strike of the orebody is 70°, the dip is 340°, the average dip is 80°, and the occurrence elevation of the orebody is 210~60m. The mine design adopts the flat-bottom structure shallow hole mining method, and the middle part is mined from top to bottom. At present, the mining of No. Fe4 ore body has been basically completed, the mining of No. Fe22 ore body has been mined above +170m level, and there are still +113m and +69m level to be mined. Affected by the early mining, the office building on the west side of No. Fe22 ore body and the central feedlot are waiting for mining. The surface road at the west end of Fe4 orebody shows obvious deformation and cracking. In this paper, the influence of mining work in the +113m and +69m middle section of Fe22 orebody on the surface is analyzed under the premise of fully considering the influence of early mining. Fig.1 shows the relative position relationship between orebody and surface structures.

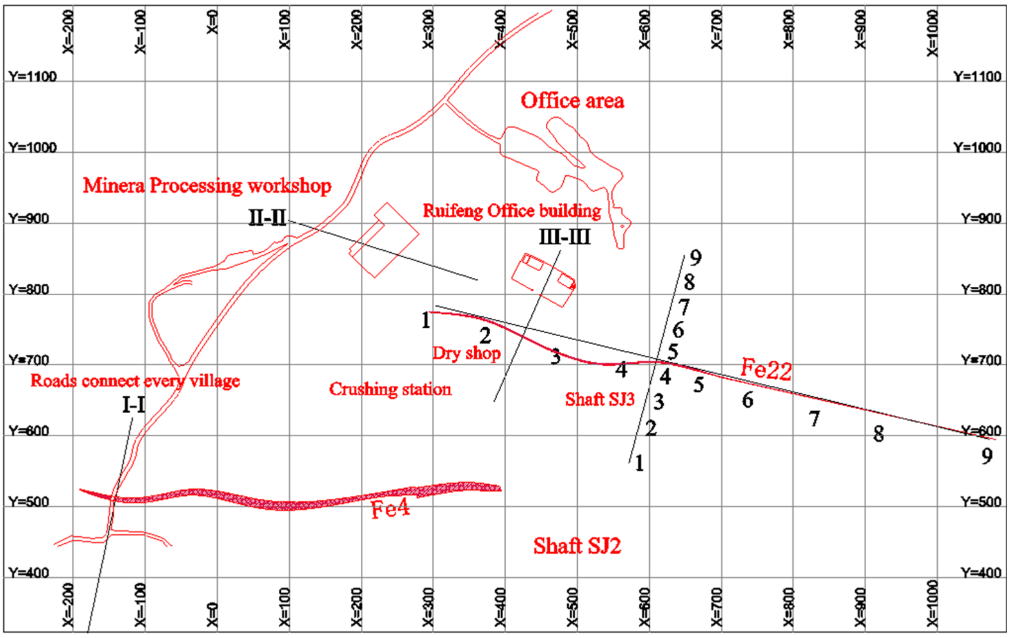

Figure 1. Relative position relationship between orebody and surface structure

3. Basis for Calculation of Surface Deformation

At present, the main indexes of the influence of surface movement and deformation on surface structures are generally recognized as surface subsidence, horizontal deformation and inclined deformation. Among them, even subsidence and horizontal movement will not cause obvious damage to buildings, etc., but when this deformation appears obvious inconsistency, surface buildings will cause obvious damage, which is mainly manifested as cracking. With reference to Modern Mining Manual edited by Wang Yunmin, the influence of deep mining on surface buildings can be analyzed by main deformation parameters shown in Fig.2.

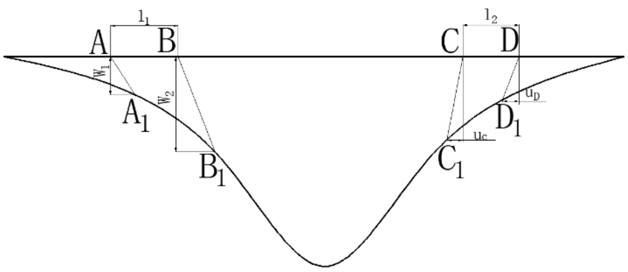

Figure 2. Schematic diagram of surface inclination and horizontal deformation

Then, surface inclination (i) is the slope value of the surface subsidence basin along a certain direction, and its average value is the subsidence difference between two points divided by the horizontal distance between two points, namely:

$$\mathrm{i}_{AB} = (W_2 - W_1) / l_1 (mm / m) \tag{1}$$

Surface horizontal deformation (ε) is the ratio of the difference in horizontal movement between the two ends of a line segment and the length of the line segment in a moving basin, the average of which is:

$$\varepsilon_{CD} = (\mathrm{u}_C - \mathrm{u}_D) / l_2 (mm / m) \tag{2}$$

4. Numerical Simulation Analysis of Surface Deformation

4.1. Construction of Engineering Geological Model and Selection of Mechanical Parameters

According to the occurrence characteristics of Fe4 ore body and Fe22 ore body, the roadway and stope structures are simplified respectively according to the actual dimensions, considering the surface topography characteristics. It is assumed that the ore body and surrounding rock are locally homogeneous and isotropic materials, and only the faults near the ore body are included in the model, while other fracture zones are not reflected in the model. Finally, a three-dimensional engineering geological model was established for the Lidigou mining area of Tangjiazhuang Iron Mine. The dimensions of the model were 2500m (-500,2000) in the x direction, 1500m (0,1500) in the y direction, and 1400m (-800,600) in the z direction, including 2984489 grids and 518339 nodes. The specific model grid and the ore body grid division are shown in Fig.3.

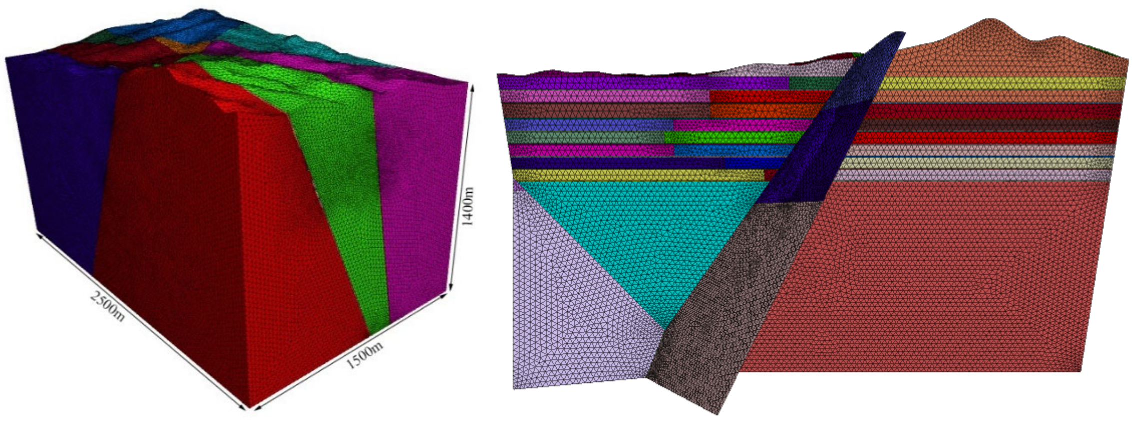

(a) Model grid (b) Orebody grid

Figure 3. Model grid and ore body grid division

Before the implementation of the numerical simulation, it is assumed that the rock mass is an ideal elastic-plastic body, and the strength and volume of the material do not change with the plastic flow after the yield point. In addition, it is assumed that there is no influence of tectonic activities in the calculation range, the in-situ stress of the original rock is geostatic field type, the contact between the rock strata is integrated, and the interior of the rock strata is a continuous medium. Based on this, Mohr-Coulomb yield criterion was selected in the calculation process, and various rock mass mechanical parameters and filling material parameters were obtained through laboratory tests, as shown in Tab.1 and Tab.2.

Table 1. Mechanical parameters of mine rock mass

lithology	Rock mass density /g·cm^{-3}	Cohesion /MPa	Internal friction Angle /°	Tensile strength /MPa	Deformation modulus /GPa	Poisson's ratio
Ore body	3.27	2.498	42.39	0.286	18.24	0.249
Surrounding rock	2.75	3.520	41.39	0.553	17.30	0.246

Table 2. Mechanical parameters of filling materials

lithology	Rock mass density /g·cm^{-3}	Cohesion /MPa	Internal friction Angle /°	Tensile strength /MPa	Deformation modulus /GPa	Poisson's ratio
Waste rock	2.30	0.70	25.00	0	0.50	0.30

According to the needs of the research work, the model size is much larger than the ore body size, and it can be considered that the model boundary far from the ore body is basically under the primary rock stress or the influence is small and negligible. Therefore, each distant boundary can be fixed, focusing only on the displacement and deformation at the top and inside of the model. Based on the established model coordinates, the displacement in x direction is fixed as 0 at x=-500m and x=2000m planes. The displacement in y direction is 0 when y=0m and y=1500m planes are fixed. At the bottom of the model z=-800m, the displacements in x, y and z directions are all 0. Because the model is only subject to gravity stress, and the displacement and deformation law of the surface should be studied, the surface of the ground is not constrained by its displacement and can be deformed freely.

4.2. Simulation of the Current Situation of Initial Surface Deformation

According to the foregoing, the mining of No. Fe4 ore body has been completed and all the waste rock is used for backfilling; all the mining of the ore body above the middle 155m level of Fe22 ore body has been completed, and the mining of the middle 113m level and the middle 69m level has not been implemented. According to the organization and management mode of mining work in the early stage of the mine, the mining order in the middle part of the mine is top-down, and the pillar is recovered after returning to the mining room in the middle part. The numerical simulation work is carried out according to the above mining process until it is consistent with the current situation of the mine. The numerical simulation results are obtained along the vertical Fe4 ore body and across the surface road direction (I-I). The typical section was intercepted along the strike direction of Fe22 ore body and through the office building (II-II), and along the vertical strike direction of Fe22 ore body and through the feedlot (III-III), and the displacement cloud map in each direction was obtained as shown in Figure 4.

Based on the above profile displacement cloud map, extract the displacement values of the key points at the corresponding locations. It can be seen that the maximum horizontal displacement and maximum vertical displacement of the area where the road is located in the I-i profile is about 44.37mm and 30.28mm respectively. The horizontal distance from this location to Fe4 orebody is about 10m, and the horizontal deformation at this location is about 4.44mm/m. The inclined deformation is about 3.03mm/m. The maximum horizontal displacement of the office building in section II-II is about 40mm, and the maximum vertical displacement is about 100mm. The horizontal distance from the position to the Fe22 orebody is about 25m. The horizontal deformation at this position is about 1.8mm/m, and the inclined deformation is about 4.0mm/m. The maximum horizontal displacement and maximum vertical displacement of the feedlot location in section III-III are about 30mm and 20mm respectively. The horizontal distance from the feedlot location is about 10m, and the horizontal deformation and inclined deformation at this location are about 3.0mm/m and 2.0mm/m respectively. With reference to the deformation requirements of the protection level of Class I buildings in the Non-Ferrous Metal Mining Design Regulations, the deformation situation of each characteristic area is shown in Tab.3.

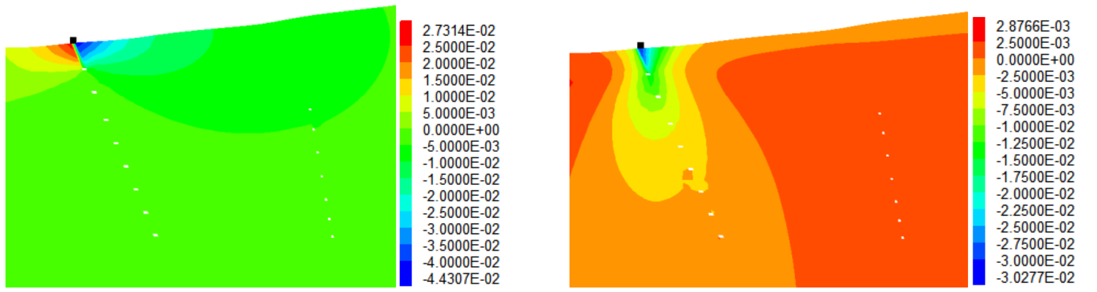

Y direction Z direction

(a)Section I-I

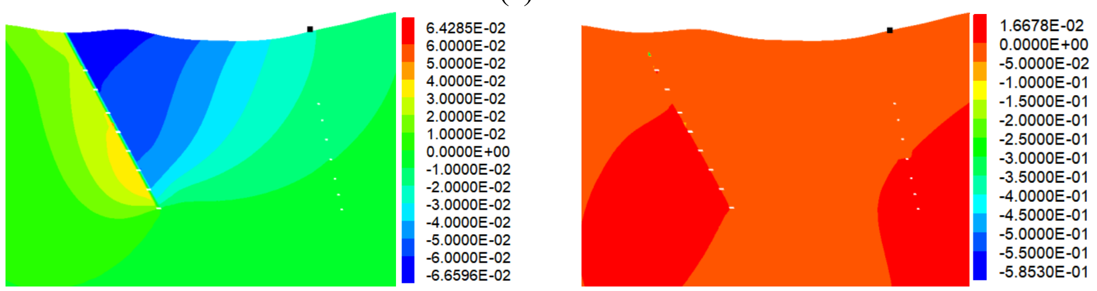

Y direction Z direction

(b)Section II-II

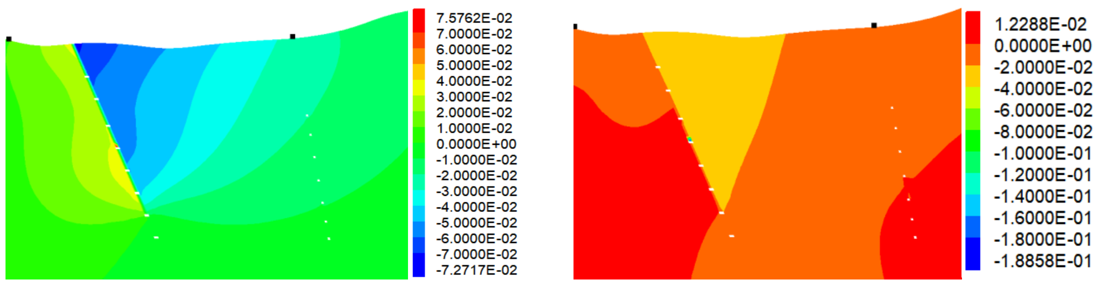

Y direction Z direction

(c)Section III-III

Figure 4. Displacement cloud images of each typical section

Taable 3. Simulation results of initial surface deformation status

Surface feature structures	**Profile name**	**Surface displacement**		**Specification requirement**		**Whether it meets the specification requirements**	**Field consistency**
		Tilt /mm/m	**Horizontal deformation /mm/m**	**Tilt /mm/m**	**Horizontal deformation /mm/m**		
Surface highway	I - I	3.03	4.44			no	is
Office building	II - II	4.00	1.80	< 3.00	< 2.00	no	is
Breeding farm	III - III	2.00	3.00			no	is

According to the numerical calculation model established above, the numerical simulation work was completed in accordance with the established mining simulation sequence, and the deformation of the characteristic position as shown in Tab.3 was obtained, which was overall consistent with the cracking characteristics displayed by the on-site structures.

4.3. Analysis of Surface Deformation Characteristics During Mining

Based on the initial simulation conditions of the mining status quo above, aiming at the surface deformation that may be induced by the mining process in the 113m and 69m middle section of Fe22 orebody, this paper completes the mining simulation of the above two middle sections in turn according to the established mining sequence, in which the pillars are not mined and the mining rooms are filled with waste rock. After the simulation is completed, The displacement cloud maps of the surface in all directions are obtained, as shown in Fig.5.

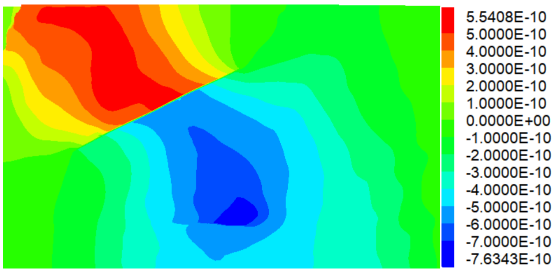

(a)X direction

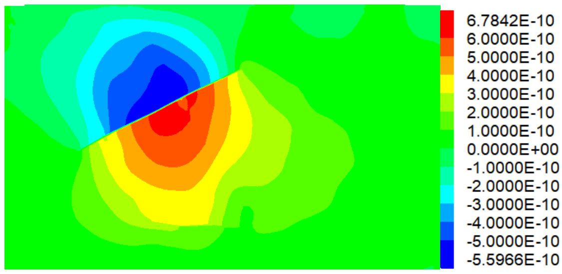

(b)Y direction

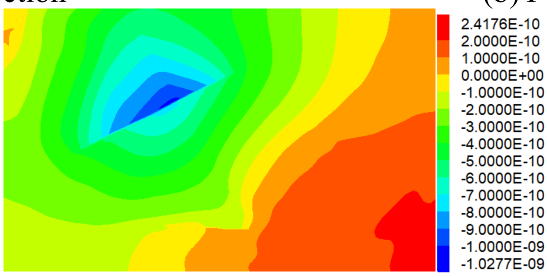

(c)Z direction

Figure 5. Surface displacement cloud map

According to the displacement cloud map of surface in all directions obtained by the above calculation, the displacement values of key points were extracted along the strike direction and vertical strike direction of the main mining area of Fe22 orebody respectively, and the horizontal and inclined deformation were calculated, as shown in Tab.4.

Taable 4. Displacement statistics of key points in each section of the surface

Profile position	Dot mark	X direction /m	In the Y direction /m	Z direction /m	Horizontal deformation /mm/m	Tilt deformation /mm/m
Along orebody strike	one	1.64 e-10	4.73 e-11	4.06 e-10	1.08 e-12	1.35 e-12
	2	1.92 e-10	2.33 e-10	6.42 e-10	5.60 e-12	6.50 e-13
	3	3.55 e-10	4.38 e-10	5.41 e-10	1.18 e-12	3.21 e-13
	4	4.73 e-10	5.91 e-10	5.94 e-10	6.54 e-13	3.48 e-13
	5	5.83 e-10	5.83 e-10	5.35 e-10	7.13 e-13	8.30 e-13
	6	5.96 e-10	4.45 e-10	3.73 e-10	8.45 e-13	9.33 e-13
	7	5.62 e-10	3.21 e-10	2.32 e-10	5.86 e-13	7.84 e-13
	8	5.00 e-10	2.29 e-10	8.24 e-11	7.14 e-13	6.80 e-13
	9	4.15 e-10	1.69 e-10	1.63 e-11	7.05 e-13	3.98 e-13
Vertical orebody strike	one	7.44 e-10	1.03 e-10	1.54 e-10	2.94 e-13	4.14 e-14
	2	-7.21 E-10	1.20 e-10	1.49 e-10	9.50 E - 13	1.20 e-13
	3	6.56 e-10	2.18 e-10	1.35 e-10	7.12 e-13	5.28 e-13
	4	5.94 e-10	3.26 e-10	2.27 e-10	4.00 e-13	5.00 e-13
	5	5.71 e-10	3.46 e-10	2.66 e-10	4.16 e-13	5.29 e-13
	6	5.32 e-10	3.56 e-10	3.16 e-10	7.75 e-13	7.06 e-13
	7	4.76 e-10	3.52 e-10	3.68 e-10	1.32 e-12	4.78 e-13
	8	3.11 e-10	2.88 e-10	4.32 e-10	2.74 e-12	2.17 e-13
	9	2.37 e-11	3.70 e-11	4.62 e-10	2.69 e-13	4.27 e-13

According to the statistical data in Table 4, the surface deformation trend along the ore body strike direction and vertical ore body strike direction can be obtained, as shown in Fig.6.

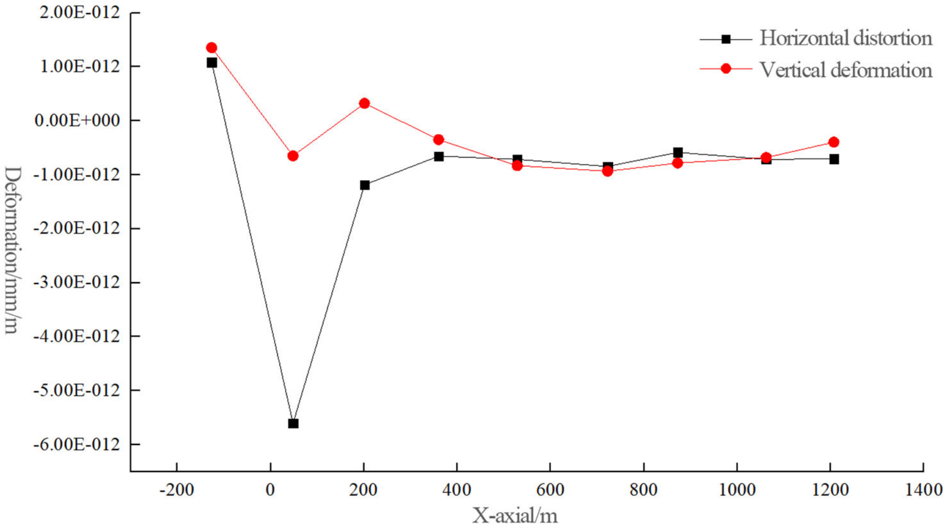

(a) Surface deformation trend along the ore body strike direction

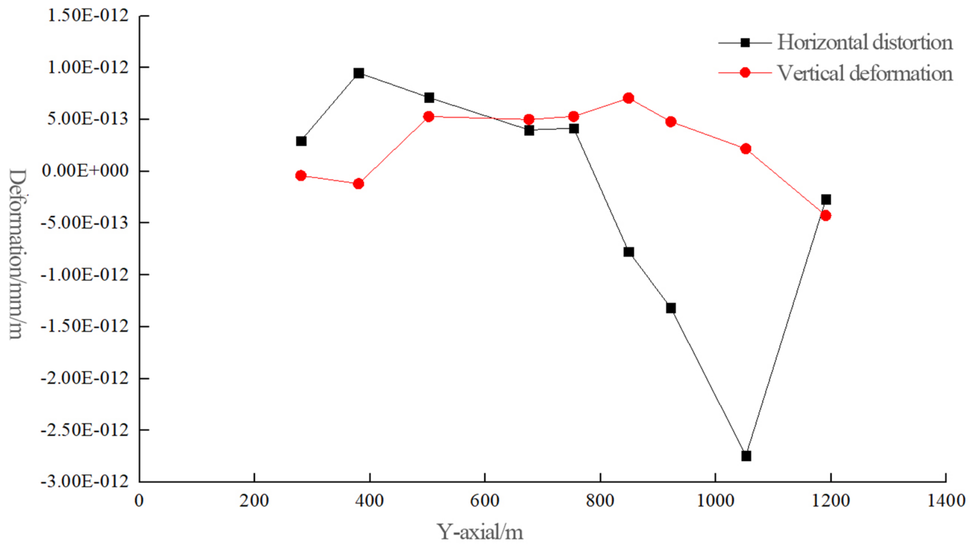

(b) Surface deformation trend in the direction of vertical ore body strike

Figure 6. Statistical chart of surface deformation trend

According to the statistical results in Figure 6, the maximum horizontal deformation of the surface is about 5.60×10-12mm/m, and the maximum inclined deformation is about 1.35×10-12mm/m, which can meet the requirements of the specification. The main deformation is compressive deformation along the strike direction of the ore body, the main deformation is tensile deformation on the upper wall of the ore body and compression deformation on the lower wall of the ore body. According to the statistical results of inclined deformation, affected by the fault plane along the direction of the ore body, the fault plane inclines to the right on the left side of the fault plane, the fault plane inclines to the left on the right side of the fault plane to the mining area, and the overmining area inclines to the right as a whole. In the vertical direction of the ore body, the upper wall of the ore body leans to the right, and the lower wall of the ore body leans first to the right and then to the left due to the influence of the fault surface.

5. Conclusion

Based on the conditions of the main mining body of Tangjiazhuang Iron Mine and the spatial position relationship between each ore body and the surface structure, combined with the pre-mining process sequence and the next mining design scheme, the influence of the mining work on the surface key facilities at the current stage is constructed by numerical simulation method, and the disturbance influence of the mining work in the deep main mining section on the surface rock formation is further analyzed. The following conclusions are obtained:

(1) The deep +113m and +69m middle section of Tangjiazhuang Iron Mine only return to the mining room without mining pillars and timely use of waste rock for high-quality filling, the surface deformation induced by mining work is small, meeting the deformation requirements of the protection level of Class I buildings in the "Non-Ferrous Metal Mining Design Regulations". It will not further induce the further expansion of the deformation area of surface buildings;

(2) The overall surface horizontal deformation induced by mining in the +113m and +69m middle section of Tangjiazhuang Iron Mine is mainly compressive deformation along the ore body strike direction, tensile deformation on the upper wall and compression deformation on the lower wall of the ore body in the vertical ore body strike direction;

(3) The surface inclined deformation induced by mining at +113m and +69m depth in Jiazhuang Iron Mine as a whole is affected by the fault as it inclinates to the right on the left side of the fault plane along the direction of ore body, to the left on the right side of the fault plane, to the right from the over-fault plane to the mining area, and to the right on the over-mining area. In the vertical direction of the ore body, the upper wall of the ore body leans to the right, and the lower wall of the ore body leans first to the right and then to the left due to the influence of the fault surface.

Acknowledgments

1) Project supported by the National Key Research and Development Program of China (2024YFC2909500)

2) Project supported by the Xinjiang "Tianshan Talents" the second batch of outstanding engineers (Chen Yin) training program

References

[1] Wu Aixiang, Wang Yong, Zhang Minzhe, et al. New progress and prospect of Key Technologies in underground mining of Metal Mines [J]. Metal Mine,2021,535(1):1-13.

[2] Xu Mengguo, Tan Tao, Cheng Aiping, et al. Stability analysis of caving stope in lower filling body of Chengchao Iron Mine [J]. Metal Mine,2019,515(5):14-20.

[3] Yang Yu, YU Jieyu, Wang Yu. Numerical simulation analysis of overlying rock movement in strip mining gob [J]. Chinese Journal of Geological Hazards and Control,2017,28(1):96-101.

[4] Wang Shanguo, Zheng Huaichang, Liu Zhihe, et al. Prevention and control technology of goaf group collapse in gypsum mine based on boundary wall effect [J]. Mining Research and Development, 2021, 41(9): 29-32.

[5] Shi Feng, HUANG Fkai, Wang Ping, et al. Study on surface cracking and Roof caving in overlying goaf during mining of 30# orebody in Huangshan Copper-nickel Mine [J]. Nonferrous Metals Mining Section,2020,72(1):1-5.

[6] Hu Jingyun, Li Shulin, Lin Feng, et al. Research on monitoring of overburden rock pressure and surface collapse disaster in large goaf [J]. Rock and Soil Mechanics,2014,35(4):1117-1122.

[7] Wang Wei, HE Huansha, Liu Chang. Research on surface movement law of overlying orebody mining in filling station [J]. Mining Research and Development,2021,41(7):66-70.

[8] Cao Wenlong, WANG Xueyan, Cao Mingqi. Analysis on the impact of underground mining on the safety of surface structures and shaft [J]. Mining Research and Development,2019,39(4):17-22.

[9] Liu Huanchun, Yu Jianxin, Jiao Huazhe, et al. Study on the influence of complex gob filling mining on ground construction [J]. Metal Mine, 2019,526(4):39-45.

[10] Guo Yan-Hui, Hou Ke-Peng, Yang Zhi-Quan, et al. Influence of dip Angle on rock displacement of steep inclined orebody under tectonic stress [J]. Mining Research and Development,20,40(7):18-21.

[11] Wang Rui, Xue Yuling, Wan Shizhen, et al. Research on cumulative temporal deformation monitoring in mining area based on DInSAR technology [J]. Chemical Minerals and Processing,2021,(11):44-47.

[12] Peng Dingxiao, Li Xibing. Delineation of surface movement zone in Hongling lead-zinc Mine based on PSO-SVM combined numerical simulation [J]. Nonferrous Metals Engineering,2019,9(3):98-106.

[13] Wu Yabin, Zhang Zhibo. Study on the influence of mining and filling sequence of open stope subsequent filling method on surface deformation [J]. Mining Research and Development,20,40(7):12-17.

[14] Ye Wei, Xu Liangji. Analysis of Surface movement and deformation law of repeated mining [J]. Metal Mine,2020,530(8):188-194.